Int Journ Earth Sciences (2000) 88 : 742–751 © Springer-Verlag 2000

ORIGINAL PAPER

Y. A. Moustafa · J. Pätzold · Y. Loya · G. Wefer

Mid-Holocene stable isotope record of corals from the northern Red Sea

Received: 4 January 1999 / Accepted: 13 September 1999

Abstract We present a study based on X-ray chronologies and the stable isotopic composition of fossil *Porites* spp. corals from the northern Gulf of Aqaba (Red Sea) covering the mid-Holocene period from 5750 to 4450 ^{14}C years BP (before present). The stable oxygen and carbon isotopic compositions of five specimens reveal regular annual periodicities. Compared with modern *Porites* spp. from the same environment, the average seasonal $\delta^{18}O$ amplitude of the fossil corals is higher (by ca. 0.35–0.60‰), whereas annual growth rates are lower (by ca. 3.5 to 2 mm/year). This suggests stronger seasonality of sea surface temperatures and increased variability of the oxygen isotopic composition of the sea water due to changes in the precipitation and evaporation regime during the mid-Holocene. Most likely, summer monsoon rains reached the northern end of the Red Sea at that time. Average annual coral growth rates are diminished probably due to an increased input and resuspension of terrestrial debris to the shallow marine environment during more humid conditions. Our results corroborate published reports of paleodata and model simulations suggesting a northward migration of the African monsoon giving rise to increased seasonalities during the mid-Holocene over northeastern Africa and Arabia.

Key words African monsoon · Corals · Holocene · Northern Red Sea · Stable isotopes

Y. A. Moustafa
National Institute of Oceanography and Fisheries, Suez, Egypt

Y. A. Moustafa (✉) · J. Pätzold · G. Wefer
Fachbereich Geowissenschaften, Universität Bremen
D-28334 Bremen, Germany
e-mail: yaser@uni-bremen.de
Fax: +49-421-2183116

Y. Loya
Department of Zoology, Tel-Aviv University, I-69978 Tel-Aviv, Israel

Introduction

Stable isotopes in corals as paleoclimatic records

Coral stable isotope time series are increasingly used for climate reconstructions. Depending on the oceanographic and climatic settings, their $\delta^{18}O$ reflect variations in sea surface temperature (SST; e.g., Wefer and Berger 1991; Dunbar et al. 1994; Druffel and Griffin 1993; Wellington et al. 1996), or sea surface salinity (SSS; e.g., Cole and Fairbanks 1990; Linsley et al. 1994), or a combination of both temperature and salinity (e.g., Gagan et al. 1994; Quinn et al. 1996; Klein et al. 1997). Salinity-related effects, such as fluctuations in the patterns of rainfall, evaporation, and water mass transport, have a large impact on the $\delta^{18}O$ of coral skeletons (Beck 1998). A multi-proxy approach combining $\delta^{18}O$ and Sr/Ca ratios has already been used to deconvolute the effects of SST and SSS, especially for fossil corals (Beck et al. 1997; Gagan et al. 1998). In contrast, corals $\delta^{13}C$ is more complex and difficult to interpret. A variety of factors, such as $\delta^{13}C$ of seawater, physiological effects, growth rate, and light intensity, influence the $\delta^{13}C$ of coral skeletons (e.g., Swart 1983; Swart et al. 1996; McConnaughey 1989).

Present climate and circulation pattern

Mediterranean countries are influenced presently by the Westerlies Zone which brings rainstorms from the northern Atlantic and North Sea through Europe and the Mediterranean Sea during winter (Goodfriend 1991). This zone moves northward during summer and southward during winter. However, due to the coastline configuration of the southeastern edge of the Mediterranean Sea, the deserts of northern Egypt, Sinai, Negev, and southern Jordan lie outside the main path of the rainstorms coming from the west (Is-

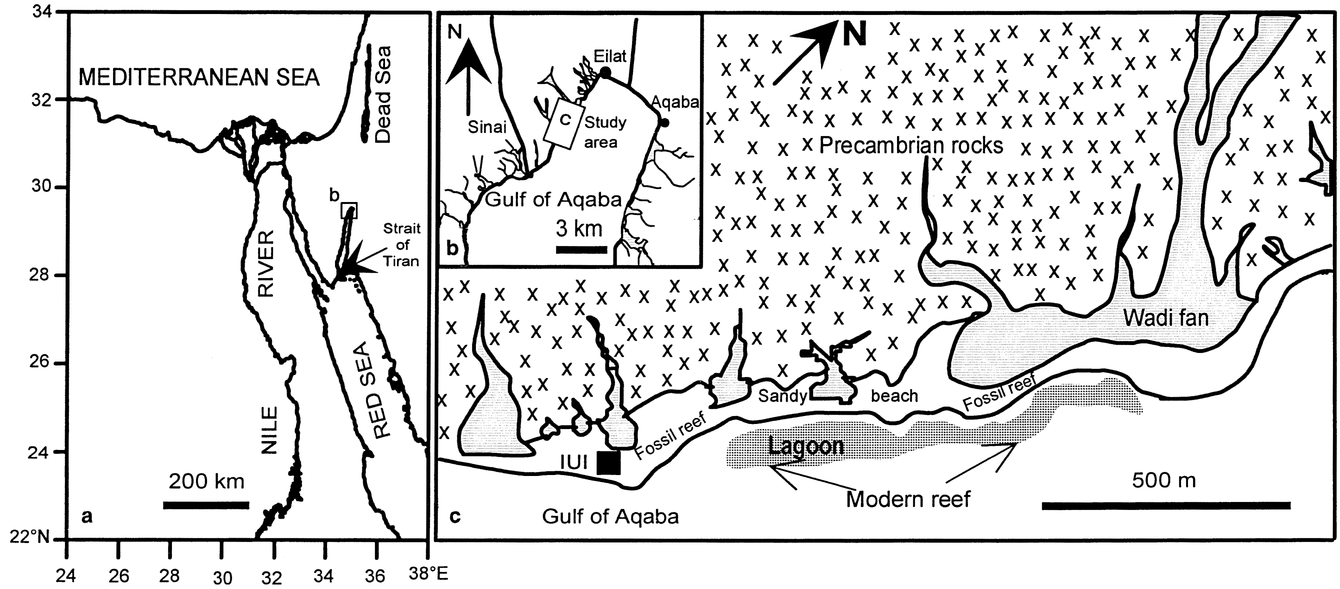

Fig. 1 **a** Location map of the northern end of the Gulf of Aqaba, **b** study area southwest of Eilat, and **c** geomorphological features adjacent to the modern and fossil reefs next to the Inter-University Institute (*IUI*)

sar 1990). The mean annual rainfall in the northern Gulf of Aqaba at Eilat is 22 mm/year (Friedman 1968) with extremes ranging between 0 and 70 mm/year (Mergner and Schuhmacher 1974). Rain only falls in winter months between November and March. The scarcity and randomness of the rains at Eilat is due to the local topography. The Dead Sea rift valley (Fig. 1a) receives a minor amount of rain coming from the Mediterranean Sea and is therefore relatively arid, whereas the adjacent mountains receive more rain and snow in winter (Issar 1990). The impact of winter rains is high as evaporation is relatively low during this season. On the contrary, under the arid and hot conditions of the Gulf of Aqaba, evaporation is extremely high (3650 mm/year) and greatly exceeds precipitation (Reiss and Hottinger 1984). Seasonal SST off Eilat range between a minimum of approximately 21 °C in winter (February to March) and a maximum of approximately 26 °C in summer (August to September). The average salinity is approximately 40.5‰. The cloud cover in Eilat is low throughout the year. The water circulation in the Gulf of Aqaba is mainly thermohaline, determined by evaporative loss and buoyancy flux. Throughout the year a considerable volume of warm, relatively low saline and highly oxygenated waters enter the Gulf of Aqaba from the Red Sea through the Strait of Tiran (Fig. 1a) and flow northward against the prevailing winds. Cooling and evaporation in the northern sector of the Gulf leads to a deeper, southward return flow of denser waters into the Red Sea (Klinker et al. 1976; Reiss and Hottinger 1984).

The African monsoon and climate during the mid-Holocene

The Holocene climatic optimum in north Africa and Saudi Arabia has been identified as a humid period between 8 and 5 ka BP (Gasse and Dodo 1997; Glennie et al. 1994). Paleolake studies as well as geomorphological and biostratigraphic data indicate that the Sahara was considerably more humid than at present. Extensive vegetation has been reconstructed for the early to mid-Holocene. This has commonly been attributed to a northward shift of the monsoonal circulation during the period of maximum summer solar radiation in the Northern Hemisphere, resulting in enhanced summer precipitation over north Africa (Harrison et al. 1997). According to the results of the Paleoclimate Modelling Intercomparison Project (PMIP) which studied the mid-Holocene African monsoon changes, the amplification of the temperature seasonal cycle for the northern continents is a direct response to the insolation forcing (Braconnot et al. 1997). Ritchie et al. (1985) suggested a humid tropical climate with annual monsoonal rainfall of at least 400 mm during mid-Holocene based on sediment and pollen evidence from the eastern Sahara. A progressive increase in aridity with annual precipitation declining from 300 mm at 6000 years BP to less than 100 mm at 4500 years BP were deduced. Presently, the amount of rainfall in the eastern Sahara ranges between 0 and 5 mm/year.

The COHMAP Members (1988) concluded that the north African–Eurasian landmass was 2–4 °C warmer during mid-Holocene than at present, which enhanced the land–ocean thermal contrast and strengthened the monsoonal rainfall over the Sahara, Arabia, and southern and eastern Asia. Lorenz et al. (1996) modelled summer and winter temperatures for the Holocene climate optimum at 6000 years BP, and suggested that summer temperature increased by 2 °C and winter temperatures were generally lower by approximately 2 °C particularly in northern Africa and Arabia. Flohn (1991) stated that the end of the mid-Holocene moist period in the Near East should have been accompanied by the end of occasional rainfall during summer half-year, reaching the Negev from the south.

Materials and methods

Fossil coral samples were taken from the top of an exposed Holocene reef terrace at approximately 2 m above present sea level and approximately 200 m distance from the present shoreline near the Inter University Institute (IUI), which is located approximately 6 km south of the City of Eilat (Israel) at the northwestern end of the Gulf of Aqaba at 29°31′N and 34°56′E (Fig. 1b, c). Ten fossil coral colonies were dated by AMS ^{14}C. The measurements were performed at the Leibniz Laboratory for Radionuclide Dating and Isotope Research, Christian Albrechts University (Kiel, Germany), for samples H2 and F3. All other samples were measured at the Center for Isotope Research, University of Groningen (Netherlands). The ^{14}C ages were corrected for isotopic fractionation with ^{13}C values as measured by AMS. The data were not corrected for possible reservoir effects. Taking into account changes in total dissolved inorganic carbon (TC) and estimates of primary production, aging time of water below the thermocline in the central part of the Gulf is calculated to be in the range of 0.5–2 years (Shemesh et al. 1994).

The coral colonies were cut into slabs approximately 5 mm thick parallel to the dominant axis of growth. The slabs were X-rayed using a cabinet X-ray system (Faxitron 43855A, Hewlett Packard, USA) in order to visualize the density growth patterns. The coral slabs were exposured at 45 kV, 3 mA, for approximately 10 min. The X-radiographs revealed regular and well-developed annual density patterns of alternating bands of high and low density (for method see, e.g., Knutson et al. 1972; Hudson et al. 1976).

A set of five coral colonies were selected for further analysis. The mineralogy of these coral samples were determined by X-ray diffraction analysis on a Philips PW 1800 (Philips, Eindhoven, The Netherlands) X-ray diffractometer (Cu, 45 kV, 35 mA) at an angle between 20 and 50° (2θ) with 1/4° 2θ per min (2 h) at the Mineralogical Section of the Geoscience Department of the University of Bremen (Germany). Samples for X-ray diffraction analysis were taken from the same region where isotope samples were drilled later.

For stable oxygen and carbon isotopic analyses the coral colonies (F8, F3, H2, H5, and F24) were sampled at high resolution along the growth direction. The samples were taken by grinding a channel into the slabs at regular intervals between 0.3 and 0.6 mm depending on bandwidth. A dental drill with a 0.6-mm diameter rounded (flower-shaped) bit was used. The drilling depth was approximately 2 mm. An example of such an isotopic profile is indicated in the X-ray of sample no. H2 (4600 ± 50 years BP; Fig. *2*).

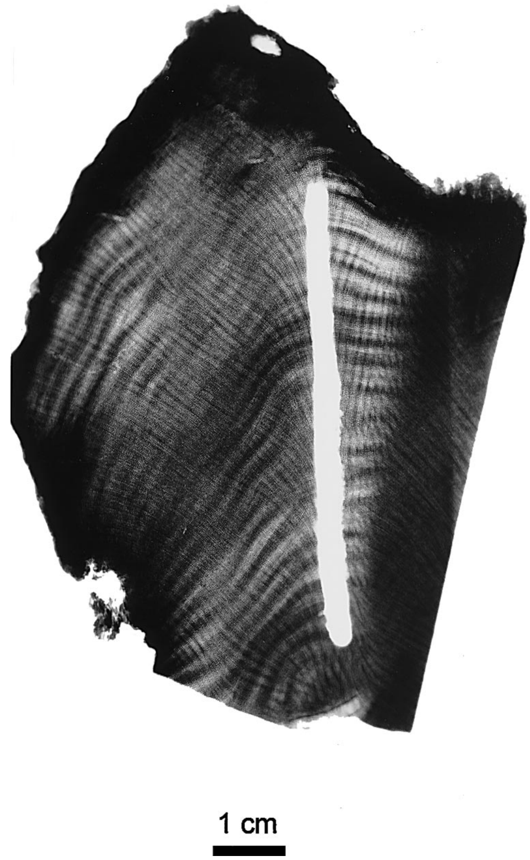

Fig. 2 Example of an X-ray of a fossil coral (H2, 4600 ± 50 ^{14}C years BP) colony. The alternating growth bands of high (*dark bands*) and low density (*light bands*) are seen. The sampling profile for stable isotope measurements is indicated by a *white line*

For stable oxygen and carbon isotopic analyses powdered carbonate samples were reacted with 100% orthophosphoric acid at 75 °C to produce carbon dioxide. The isotope measurements were performed using an automated carbonate preparation device attached to a Finnigan MAT 251 (Finnigan, Bremen, Germany) mass spectrometer. Results are given in the conventional δ notation relative to the PDB (Belemnite from the Pee Dee Formation of South Carolina) isotopic standard, calibrated by means of the NBS 19 standard:

$$\delta^{18}O(‰) = \{[(^{18}O/^{16}O)_{sample} - (^{18}O/^{16}O)_{standard}]/(^{18}O/^{16}O)_{standard}\} \times 1000$$

$$\delta^{13}C(‰) = \{[(^{13}C/^{12}C)_{sample} - (^{13}C/^{12}C)_{standard}]/(^{13}O/^{12}O)_{standard}\} \times 1000.$$

The precision based on replicate measurements of an internal laboratory standard (Solnhofen limestone of 63–80 μm) was ± 0.07 ‰ for $\delta^{18}O$ and ± 0.05 ‰ for

$\delta^{13}C$. All stable isotope analyses were carried out at the Isotope Laboratory of the Geoscience Department of the University of Bremen (Germany).

Results

^{14}C dating

The AMS ^{14}C ages of ten fossil corals (*Porites* spp.) ranged between 4450 and 5750 years BP (Table 1). This reef terrace shows the same age as many other elevated terraces along the northern Red Sea (e.g., Dabbagh et al. 1984; Al-Rifaii and Cherif 1988; Dullo 1990; Gvirtzman et al. 1992; Gvirtzman 1994). Friedman (1965) described samples from a fossil reef southwest of Eilat having approximately the same age (4770 ± 140 years BP).

Table 1 AMS ^{14}C ages of fossil coral colonies from Eilat, northern end of the Gulf of Aqaba. The datings were performed at the Leibniz-Labor (KIA) in Kiel, Germany, and the Center for Isotope Research (GrA) Groningen, Netherlands

	Sample identification	Lab no.	^{14}C-Age (years BP)
1	H2	KIA 1881	4600 ± 50
2	F3	KIA 1882	4890 ± 40
3	H5	GrA 7840	4600 ± 60
4	F6	GrA 7824	4960 ± 60
5	F7	GrA 7825	5140 ± 60
6	F8	GrA 7827	5750 ± 60
7	F9	GrA 7829	5100 ± 60
8	F11	GrA 7830	5370 ± 60
9	F23	GrA 7832	4920 ± 90
10	F24	GrA 7833	4450 ± 60

X-ray diffractometry

X-ray diffractometry shows that most samples are still aragonitic in composition, except for sample F24 (4450 ± 60 years BP) which contains traces of calcite. We conclude that the samples were not subject to diagenetic alterations, which might have increased ^{14}C content. In addition, the aragonitic minerology is taken as evidence that the stable isotopic composition has not been altered and can thus be used for paleoclimatic reconstructions.

Growth rates

The X-rays of our coral colonies reveal continuous growth records of up to 18 years. The annual growth rates were determined from the seasonal cycles of the stable oxygen isotopes. Despite low annual growth rates, our drilling technique allowed a nearly monthly sampling resolution (Fig. 3). The mid-Holocene corals show lower mean annual growth rates (between 3.4 ± 0.7 and 5.7 ± 1.4 mm/year) than corals from the modern reef environment at Eilat (between 7.1 ± 1.9 and 7.9 ± 1.6 mm/year), except for colony F8 (7.2 ± 1.5 mm/year at 5750 ± 60 years BP) which has annual growth rates comparable to the modern colonies (Fig. 4a). At the northeastern coast of the Gulf of Aqaba, adjacent to the City of Aqaba, modern corals reveal even higher growth rates. Corals from water depths between 2 and 7 m grow at rates between 8.7 (± 1.4) and 14.4 (± 1.2) mm/year (Heiss 1996). Local effects in the circulation pattern at the northern end of the Gulf seem to be responsible for these differences in growth rate. Whereas the reefs off Aqaba are locally affected by upwelling of water masses, downwelling occurs in front of the reefs at Eilat (Mergener and Schuhmacher 1974; Genin et al. 1995). Increased plankton abundance in the upwelling area off Aqaba seems to favor the coral reef growth.

Stable isotope analyses

Stable oxygen isotopes

Five *Porites* spp. (F8, F3, H2, H5 and F24) colonies were studied for stable carbon and oxygen isotope composition. The lengths of the isotope records records vary between 9 and 18 years. The isotopic records of two modern corals are also for reference (Fig. 3; Klein et al. 1992; Felis et al. 1998b). All mid-Holocene colonies show clear seasonal variations. The stable oxygen isotope data are summarized in Table 2. The values of the fossil corals are heavier (between −2.13 and −2.76 ‰ on average) compared with the modern corals (−2.77 and −3.04‰ on average) and the mean seasonal $\delta^{18}O$ amplitudes (difference between minima and maxima) of the mid-Holocene corals (between 1.1 and 1.35‰) is greater than in modern corals (between 0.71 and 0.75‰; Figs. 4, 5). Samples drilled in high-density bands were found to be enriched in $\delta^{18}O$ compared with low-density bands. We conclude that the high-density bands were deposited during winter, whereas the low-density bands were deposited during summer. This density pattern is similar to that of modern *Porites lobata* (3 m water depth) from Eilat (Klein et al. 1992; Klein et al. 1993) and modern *Porites* spp. (4.5 m water depth) from Aqaba (Heiss 1994).

Stable carbon isotopes

The carbon isotope composition shows distinct annual periodicity (Fig. 3), although it is less well developed in the colonies F8 and H2. The seasonal amplitudes of

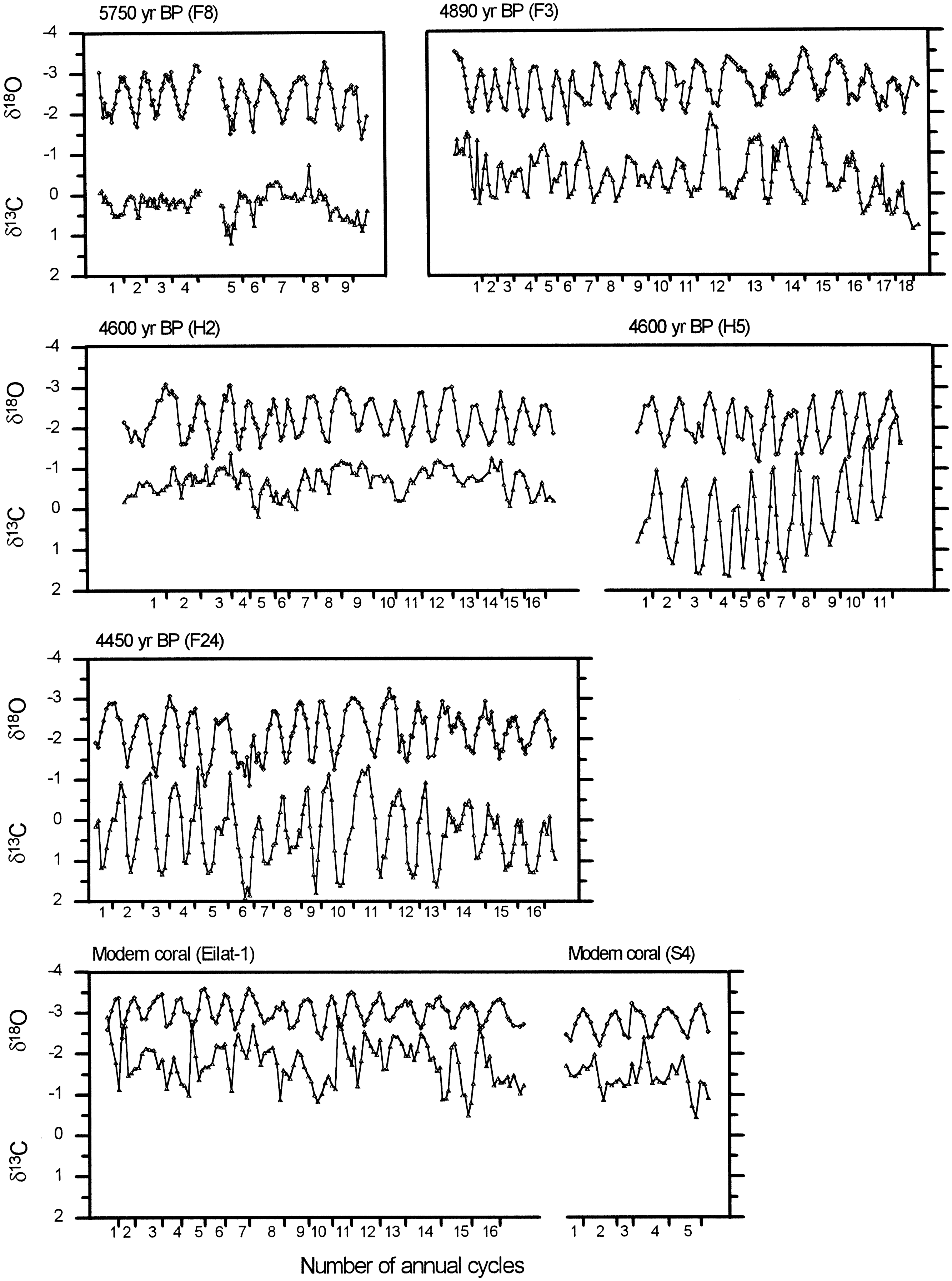
5750 yr BP (F8)
4890 yr BP (F3)
4600 yr BP (H2)
4600 yr BP (H5)
4450 yr BP (F24)
Modern coral (Eilat-1)
Modern coral (S4)
δ18O
δ13C
Number of annual cycles

Table 2 Summary of statistics for stable oxygen isotope analyses of mid-Holocene and modern corals from Eilat, northern Gulf of Aqaba

$\delta^{18}O$ (‰PDB)	Maximum	Minimum	Range	Mean	SD	Sample
F8 (5750 year BP)	−1.39	−3.27	1.89	−2.41	0.44	127
F3 (4890 year BP)	−1.75	−3.57	1.82	−2.67	0.42	192
H2 (4600 year BP)	−1.27	−3.09	1.82	−2.24	0.45	150
H5 (4600 year BP)	−1.16	−2.90	1.74	−2.13	0.48	75
F24 (4450 year BP)	−1.45	−2.94	1.49	−2.21	0.39	190
S4 (Modern)[a]	−2.19	−3.22	1.03	−2.77	0.29	35
Eilat-1 (Modern)[b]	−2.37	−3.59	1.22	−3.04	0.28	121

[a] Data from Klein et al. (1992)
[b] Data from Felis et al. (1998b)

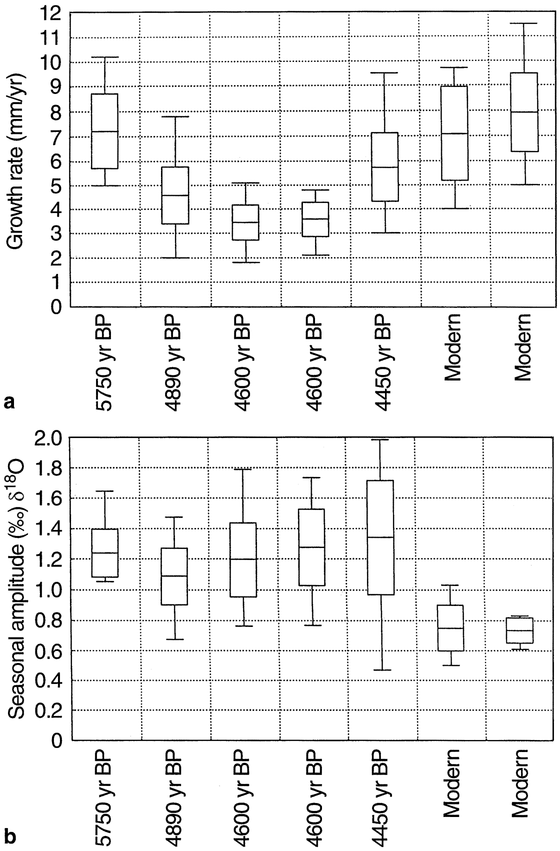

Fig. 4 **a** Box plot of growth rate of fossil and modern coral samples showing the mean, mean ± standard deviation (1 σ), minimum, and maximum growth rate of each sample. The mean growth rate of the fossil samples are lower than that of the modern corals. Note that the growth rates of the corals from 4600 year BP have the same mean and ranges. **b** Box plot of $\delta^{18}O$ seasonal amplitude in fossil and modern coral samples showing the mean, mean ± standard deviation (1 σ), minimum, and maximum seasonal amplitude for each sample. The mean seasonal amplitude of fossil corals are clearly higher than for modern corals

Fig. 3 The stable oxygen (*upper line*) and carbon (*lower line*) isotopic compositions and time series of five fossil corals from the mid-Holocene years BP and two modern corals from the northern Red Sea (S4 from Klein et al. 1992; Eilat-1 from Felis et al. 1998b). The growth direction is from left to right

$\delta^{13}C$ (Table 3) are much more variable than in oxygen isotope cycles. Generally, the mid-Holocene colonies show heavier values in $\delta^{13}C$ (between −0.68 and 0.46 ‰ on average) than modern corals (between −1.78 and −1.42 ‰ on average). The phase relationship between carbon and oxygen isotopes is very similar in fossil and modern records. Figure 3 shows that the most positive $\delta^{13}C$ values generally lag the most positive $\delta^{18}O$ values by approximately 2–3 months, and that minimum $\delta^{13}C$ occur during autumn or winter.

Discussion

The $\delta^{18}O$ of marine organisms varies as a function of the $\delta^{18}O/\delta^{16}O$ ratio of seawater and temperature (Epstein et al. 1953; Wefer and Berger 1991). The oxygen isotopic ratio of ocean surface water reveals spatial and temporal variability which is linked to changes in evaporation, precipitation, and to atmospheric and oceanic water mass transport (e.g., Rohling and Bigg 1998). Thus, it is closely connected to changes in SSS. The oxygen isotope ratios of coral aragonite skeletons are not secreted in equilibrium with the surrounding seawater, but exhibit biological depletion of ^{18}O during calcification. This "vital effect" seems to be species dependent and is more or less constant. Thus,

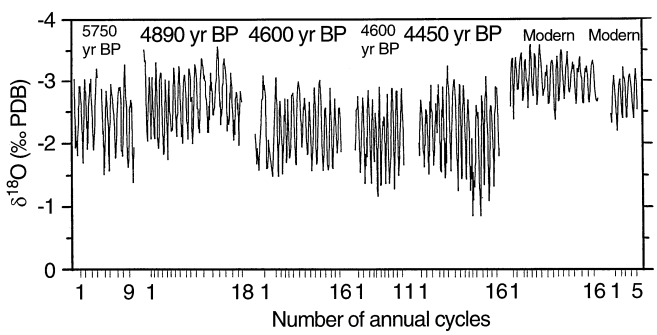

Fig. 5 Stable oxygen isotope time series from fossil (4450–5750 ^{14}C years BP)and modern corals. The fossil corals show a considerably higher seasonal $\delta^{18}O$ amplitude (ca. 1.7 times) as well as heaiver mean $\delta^{18}O$ (ca. 0.5‰) compared with modern corals from the same location (Klein et al. 1992; Felis et al. 1998b)

Table 3 Summary of statistics for stable carbon isotope analysis of mid-Holocene and modern corals from Eilat, northern Gulf of Aqaba

$\delta^{13}C$ (‰PDB)	Maximum	Minimum	Range	Mean	SD	Sample
F8 (5750 year BP)	1.20	−0.75	1.95	0.22	0.29	127
F3 (4890 year BP)	0.86	−1.99	2.85	−0.48	0.56	192
H2 (4600 year BP)	0.18	−1.39	1.57	−0.68	0.31	150
H5 (4600 year BP)	1.73	−2.29	4.03	0.08	1.01	75
F24 (4450 year BP)	1.64	−0.75	2.39	0.46	0.62	190
S4 (Modern)[a]	−0.44	−2.40	1.96	−1.42	0.37	35
Eilat-1 (Modern)[b]	0.44	−2.90	2.46	−1.78	0.52	121

[a] Data from Klein et al. (1992)
[b] Data from Felis et al. (1998b)

whereas absolute temperature reconstructions are uncertain, relative seasonal temperature variations can be resolved with high resolution providing there is no change in SSS (e.g., Weber and Woodhead 1972; Fairbanks and Dodge 1979; Pätzold 1984).

Modern oxygen isotope cycles of corals from Eilat do not resolve the temperature variations between approximately 21 and 26 °C (i.e., 0.9‰ in $\delta^{18}O$) due to a salinity increase during summer which dampens the isotope signal (Felis et al. 1998a). The modern seasonal salinity amplitude is 0.5‰ (Paldor and Anati 1979; Wolf-Vecht et al. 1992). This seasonal change in salinity corresponds to a change in the isotope composition of seawater, and finally results in a reduction of the coral $\delta^{18}O$ amplitude by approximately 12% in modern corals in the northern Red Sea (Felis et al. 1998a).

The fossil coral records clearly document that the seasonal cycles of oxygen isotopes in annual growth bands in the northern Red Sea were amplified during the mid-Holocene. Despite a reduction in growth rates, seasonal amplitudes of $\delta^{18}O$ cycles are enhanced in mid-Holocene corals. Due to the detailed sampling procedure, an almost monthly resolution was achieved for both fossil and modern corals. It is anticipated that this sampling procedure fully resolved the recorded seasonal isotope cycles.

Model simulations of the earth's orbital parameters demonstrate that the seasonal cycle of solar radiation was enhanced during the early and mid-Holocene in the Northern Hemisphere (Kutzbach and Street-Perrott 1985). Solar radiation was increased during summer and decreased during winter by approximately 5 and 2% at 6000 and 3000 years BP, respectively, giving rise to cooler winters and warmer summers. As a consequence the thermal contrast between Northern Hemisphere continents and the ocean increased and amplified the monsoonal circulation. A major intensification of the summer monsoon combined with increased southwesterly winds increased the transport of moisture from the oceans onto the northern land masses. More recent simulations with a climate model that asynchronously couples the atmosphere and the ocean show that summer monsoon precipitation increased as far north as 23°N and up to 30°N in northern Africa (Kutzbach and Liu 1997). The suggested lowering of SSTs in winter and increased heating during summer is consistent with our findings at 29°N. In addition, increased precipitation during the summer monsoon season will have lowered the coral oxygen isotope signal in the warm season. The difference between the average seasonal amplitudes of fossil and modern corals ranges from 0.35 to 0.6‰ which could imply an increase of seasonal SST amplitude of approximately 2–3.5 °C, if entirely related to temperature. The gradient of 0.18‰/°C (Gagan et al. 1994) is widely accepted for temperature interpretation of *Porites* $\delta^{18}O$ records (Charles et al. 1997; Felis et al. 1998a). If the change is interpreted as a pure temperature signal, it would imply lowest SST down to 15 or 16 °C, which is unrealistic since coral growth ceases at temperatures below approximately 18 °C. On the other hand, if this difference were entirely related to salinity, it would be equivalent to a 1–2‰ change in salinity (0.29‰ $\delta^{18}O$/‰ salinity; Craig 1966). The enhanced seasonal $\delta^{18}O$ signals probably reflect a combined effect of temperature and salinity. Their relative contribution, however, remains to be resolved.

A potential tool to separate temperature and salinity effects and to determine absolute SSTs is the use of an additional coral proxy thermometer. Sr/Ca ratios in corals also vary as a function of temperature. The Sr/Ca ratio of ocean water is considered constant over larger time scales, although some work suggests that ocean water also reveals variability in Sr/Ca ratio. Sr/Ca ratios of corals may also exhibit some growth rate dependence (deVilliers et al. 1995). Calibrations of the Sr/Ca thermometer reveal consistent results in many areas despite some discrepancies (deVilliers et al. 1995; Shen et al. 1996). Recent applications of a multi-proxy approach using $\delta^{18}O$ and Sr/Ca in coral skeletons provided convincing results considering paleotemperatures and variations of evaporation, precipitation, and ocean surface salinity (Gagan et al. 1998; Beck 1998). Further trace element analysis of fossil coral records from the early and late Holocene from the northern Red Sea will help to elucidate climatic changes in the Near East region.

In addition, the $\delta^{18}O$ signal of the different corals during mid-Holocene (Fig. 5) could be controlled through variations in the intensity of the SW monsoon. Many climate proxy data indicate that major changes occur at approximately 5000 year BP. After the hieroglyphical documents, the Nile floods fall as a result of the reduction of the SW summer monsoon from 3018 to 2500 years BC (ca. 4970 to 4450 years BP) in southern Egypt (Westendorf and Henfling 1989; Henfling and Pflaumbaum 1991). As a result of this reduction in the intensity of the SW monsoon, the mean $\delta^{18}O$ signal in the fossil corals have been reduced by approximately of 0.5‰ between 4890 and 4450 ^{14}C years BP (Fig. 5; Table 2). The African lakes (Ethiopian and Chad) show a decreasing in water levels between 5000 and 4000 years BP (e.g., Gasse 1977; Gasse and Street-Perrot 1978; Gillespie et al. 1983; Gasse and Van Campo 1994). Also, the Dead Sea level according to Mount Sedom caves exhibit a retread level in the same time window (Neev and Emery 1995; Frumkin 1997). During the third millennium BC, the archaeological and soil-stratigraphic data indicate a collapse of rain-fed agriculture civilisation of northern and southern Mesopotamia (i.e., Subir and Akkadian empire; Weiss et al. 1993). More recently, a study based on simulation of saharan vegetation in the mid-Holocene shows an abrupt decrease in the fraction of saharan vegetation cover between 6000 and 4000 years BP which was simulated by using an atmosphere-vegetation model (Claussen et al. 1999). All these studies may explain the change of corals $\delta^{18}O$ between 4890 and 4600 years BP. Despite the average change, the seasonal $\delta^{18}O$ of fossil corals stays amplified afterwards. This indicates that the climate between 4600 and 4450 years BP was still wetter than at present.

Changes in the absolute isotope values could also reflect changes in coral growth rate. Variations in growth and calcification rate have an impact on the fractionation of stable isotopes (Land et al. 1975; Pätzold 1986; McConnaughey 1989). A reduction in the growth rate entails heavier isotope values of oxygen and carbon. Since annual growth rates of the mid-Holocene corals were reduced by up to 45% compared with the average modern values (Fig. 4a), heavier isotope values are expected. Indeed, both oxygen and carbon isotope signals reveal heavier values in the fossil records. The reduction of coral growth during the mid-Holocene is probably triggered by increased input and resuspension of terrestrial sediments. The constant energy expenditure for removal of sediment particles and reduction of light decreases growth rate (Dodge et al. 1974). Outcrops of the Holocene reef formation at Eilat are characterized by increased interlayering of gravel deposits and intensification of beach rock formation. Both are taken as signs for more humid conditions.

The difference in the $\delta^{13}C$ fractionation between mid-Holocene and modern corals (Table 3) could be attributed to kinetic fractionation effects. McConnaughey (1989) suggested that a kinetic effect due to slow skeletal growth rate and hence reduced metabolism results in heavier $\delta^{13}C$. In the other hand, Klein et al. (1992, 1993) found the same phase relation between $\delta^{13}C$ and $\delta^{18}O$ values and explained it with the seasonal time lag between maximum light and maximum temperature. Solar irradiance in northern Red Sea reaches its minimum between December and January, whereas minimum seawater temperatures are recorded between February and March. Pätzold (1984, 1986) described a similar shift between the seasonal variation of carbon and oxygen signals of modern and fossil mid-Holocene *Porites lobata* from Cebu in the Philippines.

Conclusion

The stable isotope composition of five mid-Holocene coral colonies from the northern Gulf of Aqaba were compared with modern corals from the same environment. The results indicate that the seasonal $\delta^{18}O$ amplitude was greater than in modern corals. This is most probably due to a larger seasonal temperature contrast and a reduction of salinity during the summer season for the mid-Holocene. However, $\delta^{18}O$ alone cannot resolve the relative contribution of SST and SSS, and additional tracers are needed. Our results support the hypotheses of summer monsoon rains reaching the northern Red Sea during mid-Holocene times while seasonal solar radiation was enhanced. A climatic change seems to have occurred between approximately 4900 and 4600 years BP. This date coincides with a period of rapid fall in north African lake levels indicating reduction of moisture transport from the ocean. Enhanced seasonalities can be reconstructed at least until 4450 ^{14}C years BP.

Acknowledgements We thank T. Felis and M. Fine for the collection of the coral samples. Special thanks are due to M. Segl for performing the stable isotopic measurements and preparation of the sample for AMS ^{14}C dating. AMS ^{14}C measurements were carried out at the Leibniz Laboratory for Radionuclide Dating and Isotope Research, Christian Albrechts University (Kiel, Germany), and the Center for Isotope Research, University of Groningen (The Netherlands). All stable isotopic measurements were carried out at the isotope laboratory at Bremen University (Germany). We also thank S. Draschba, T. Felis, and H. Kuhnert for critical discussions, their help during preparation of the X-rays and guidance to take the isotope samples. J. Bijma improved the English of the manuscript. The manuscript was substantially improved by the review comments of T. Correge and C. Dullo. This work was partly supported by the "Red Sea Program" (RSP) of the "Bundesministerium für Bildung, Wissenschaft, Forschung und Technologie" (BMBF, 03F0151A6), a grant from the University of Bremen, and a grant of the Graduierten Kolleg "Stoff-Flüsse in marinen Geosystemen" funded by the Deutsche Forschungsgemeinschaft.

References

Al-Rifaii IA, Cherif OH (1988) The fossil coral reefs of Al-Aqaba, Jordan. Facies 18:219–230

Beck W (1998) Warmer and wetter 6000 years ago? Science 279:1003–1004

Beck JW, Récy J, Taylor F, Edwards RL, Cabioch G (1997) Abrupt changes in early Holocene tropical sea surface temperature derived from coral records. Nature 385:705–707

Braconnot P, Joussaume S, DeNoblet N, Ramstein G (1997) Mid-Holocene and last glacial maximum African monsoon changes as simulated within PMIP. Paleomonsoons Project Workshop at Siwa Oasis, Egypt, 11–22 January (Abstracts)

Charles CD, Hunter DE, Fairbanks RG (1997) Interaction between the ENSO and the Asian monsoon in a coral record of tropical climate. Science 260:1790–1793

Claussen M, Kubatzki C, Brovkin V, Hoelzmann P, Pachur H-J (1999) Simulation of an abrupt change in Saharan vegetation in the mid-Holocene. Geophys Res Lett 26:2037–2040

COHMAP Members (1988) Climatic changes of the last 18,000 years: observations and model simulations. Science 241:1043–1052

Cole JE, Fairbanks RG (1990) The Southern Oscillation recorded in the $\delta^{18}O$ of corals from Tarawa Atoll. Paleoceanography 5:669–683

Craig H (1966) Isotopic composition and origin of the Red Sea and Salton Sea geothermal brines. Science 154:1544–1548

Dabbagh A, Emmermann R, Hötzl H, Jado AR, Lippolt W, Kollmann W, Moser H, Rauert W, Zötl JG (1984) The development of Tihamat Asir during the Quaternary. In: Jado AR, Zötl JG (eds) Quaternary period in Saudi Arabia. Springer, Berlin Heidelberg New York, pp 150–174

DeVilliers S, Nelson BK, Chivas AR (1995) Biological controls on coral Sr/Ca and $\delta^{18}O$ reconstructions of sea surface temperatures. Science 269:1247–1249

Dodge RE, Aller RA, Thompson J (1974) Coral growth related to resuspension of bottom sediments. Nature 247:574–577

Druffel ERM, Griffin S (1993) Large variations of surface ocean radiocarbon: evidence of circulation changes in the southern Pacific. J Geophys Res 98:249–259

Dullo W-C (1990) Facies, fossil record, and age of Pleistocene reefs from the Red Sea (Saudi Arabia). Facies 22:1–46

Dunbar RB, Wellington GM, Colgan MW, Glynn PW (1994) Eastern Pacific sea surface temperature since 1600 AD: the $\delta^{18}O$ record of climate variability in Galápagos corals. Paleoceanography 9:291–315

Epstein S, Buchsbaum R, Lowenstam HA, Urey HC (1953) Revised carbonate-water isotopic temperature scale. Bull Geol Soc Am 64:1315–1325

Fairbanks RG, Dodge RE (1979) Annual periodicity of the $^{18}O/^{16}O$ and $^{13}C/^{12}C$ ratios in the coral *Montastrea annularis*. Geochim Cosmochim Acta 43:1009–1020

Felis T, Pätzold J, Wefer G, Fine M, Loya Y, Nawar AH (1998a) First results of a coral-based history of recent climate in the northern Red Sea. Zbl Geol Paläont Teil 1 H1/2:197–207

Felis T, Pätzold J, Wefer G, Loya Y (1998b) Vertical mixing and plankton blooms recorded in coral skeletal carbon isotopes. J Geophys Res 103:731–740

Flohn H (1991) Towards a physical interpretation of the end of the Holocene moist period in the Near East. Erdkunde 45:163–167

Friedman GM (1965) A fossil shoreline reef in the Gulf of Elat (Aqaba). Isr J Earth Sci 14:86–90

Friedman GM (1968) Occurrence and stability relationships of aragonite, high-magnesium calcite under deep-sea conditions. Geol Soc Am Bull 76:1191–1196

Frumkin A (1997) The Holocene histroy of Dead Sea levels. In: Niemi TM, Ben-Avraham Z, Gat JR (eds) The Dead Sea: the lake and its setting. Oxford University Press, New York, pp 237–248

Gagan MK, Chivas AR, Isdale PJ (1994) High-resolution isotopic records from corals using ocean temperature and mass spawning chronometers. Earth Planet Sci Lett 121:549–558

Gagan MK, Ayliffe LK, Hopley D, Cali JA, Mortimer GE, Chappell J, McCulloch MT, Head MJ (1998) Temperature and surface-ocean water balance of the mid-Holocene tropical western Pacific. Science 279:1014–1018

Gasse F (1977) Evolution of lake Abhé (Ethiopia and T.F.A.I.) from 70,000 B.P. Nature 2:42–45

Gasse F, Dodo A (1997) Combined surface and groundwater palaeohydrology in the Sahara and the Sahel for understanding past climate change. Paleomonsoons Project Workshop at Siwa Oasis Egypt 11–22 January (Abstracts)

Gasse F, Street-Perrot FA (1978) Late Quaternary lake level fluctuations and environments of the northern rift Valley and Afar region (Ethiopia and Djibouti). Paleogeogr Paleoclimatol Paleoecol 24:279–325

Gasse F, Van Campo E (1994) Abrupt post-glacial climate events in west Asia and North Africa monsoon domains. Earth Planet Sci lett 126:435–456

Genin A, Lazar B, Brenner S (1995) Vertical mixing and coral death in the Red Sea following the eruption of Mount Pinatubo. Nature 377:507–510

Gillespie R, Street-Perrot FA, Switzur R (1983) Post-glacial arid episodes in Ethiopia have implications for climate prediction. Nature 306:680–683

Goodfriend GA (1991) Holocene trends in ^{18}O in land snail shells from the Negev Desert and their implications for changes in rainfall source areas. Quaternary Res 35:417–426

Glennie KW, Pugh JM, Goodall TM (1994) Late Quaternary Arabian Desert models of Permian Rotliegend reservoirs. Expl Bull 274:1–19

Gvirtzman G (1994) Fluctuations of the sea level during the past 400,000 years: the record of Sinai, Egypt (northern Red Sea). Coral Reefs 1:203–214

Gvirtzman G, Kronfeld J, Buchbinder B (1992) Dated coral reefs of southern Sinai (Red Sea) and their implication to late Quaternary sea levels. Mar Geol 108:29–37

Harrison SP, Kutzbach JE, Coe M, Foley J, Hoelzmann P, Jolly D, Liu Z, Prentice IC (1997) Land–ocean–atmosphere interactions and the amplification of the African monsoon in the mid-Holocene. Paleomonsoons Project Workshop at Siwa Oasis Egypt 11–22 January (Abstracts)

Heiss GA (1994) Coral reefs in the Red Sea: growth, production and stable isotopes. GEOMAR Rep 32, PhD thesis, Kiel University

Heiss GA (1996) Annual band width variation in Porites spp. from Aqaba, Gulf of Aqaba, Red Sea. Bull Mar Sci 59:393–403

Henfling E, Pflaumbaum H (1991) Neue Aspekte zur klimatischen Interpretation der hohen pharaonischen Nilflutmarken am 2. Katarakt aus ägyptologischer und geomorphologischer Sicht. Würzburg Geogr Arb 80:87–109

Hudson JH, Shinn EA, Halley RB, Lidz B (1976) Sclerochronology: a tool for interpreting past environments. Geology 4:361–364

Issar AS (1990) Water shall flow from the rock; hydrology and climate in the lands of the Bible. Springer, Berlin Heidelberg New York, pp 1–213

Klein R, Pätzold J, Wefer G, Loya Y (1992) Seasonal variations in the stable isotopic composition and the skeletal density pattern of the coral *Porites lobata* (Gulf of Eilat, Red Sea). Mar Biol 112:259–263

Klein R, Pätzold J, Wefer G, Loya Y (1993) Depth-related timing of density band formation in *Porites* spp. corals from the Red Sea inferred from X-ray chronology and stable isotope composition. Mar Ecol Prog Ser 97:99–104

Klein R, Tudhope AW, Chilcott CP, Pätzold J, Abdulkarim Z, Fine M, Fallick AE, Loya Y (1997) Evaluating southern Red Sea corals as a proxy record from the Asian monsoon. Earth Planet Sci Lett 148:381–394

Klinker J, Reiss Z, Kropach C, Levanon I, Harpaz H, Halicz E, Assaf G (1976) Observations on the circulation pattern in the Gulf of Elat (Aqaba), Red Sea. Isr J Earth Sci 25:85–103
Knutson DW, Buddemeier RW, Smith SV (1972) Coral chronometers: seasonal growth bands in reef corals. Science 177:270–272
Kutzbach JE, Liu Z (1997) Response of the African monsoon to orbital forcing and ocean feedbacks in the middle Holocene. Science 278: 440–443
Kutzbach JE, Street-Perrott FA (1985) Milankovitch forcing of fluctuations in the level of tropical lakes from 18 to 0 kyr BP. Nature 317:130–134
Land LS, Lang JC, Barnes DJ (1975) Extension rate: a primary control on the isotopic composition of West Indian (Jamaican) scleractinian reef coral skeletons. Mar Biol 33:221–233
Linsley BK, Dunbar RB, Wellington GM, Mucciarone DA (1994) A coral-based reconstruction of Intertropical Convergence Zone variability over Central America since 1707. J Geophys Res 99:9977–9994
Lorenz S, Grieger B, Helbig P, Herterich K (1996) Investigating the sensitivity of the atmospheric general circulation model ECHAM 3 to paleoclimatic boundary conditions. Geol Rundsch 85:513–524
McConnaughey T (1989) ^{13}C and ^{18}O isotopic disequilibrium in biological carbonates. I. Patterns. Geochim Cosmochim Acta 53:151–162
Mergner H, Schuhmacher H (1974) Morphologie, Ökologie und Zonierung von Korallenriffen bei Aqaba, (Golf von Aqaba, Rotes Meer). Helgoländer Wiss Meeresunters 26:238–358
Neev D, Emery KO (1995) The destruction of Sodom, Gomorrah, and Jericho: geological, climatological, and archaeological background. Oxford University Press, New York
Paldor N, Anati DA (1979) Seasonal variations of temperature and salinity in the Gulf of Elat (Aqaba). Deep-Sea Res 26:661–672
Pätzold J (1984) Growth rhythms recorded in stable isotopes and density bands in the reef coral *Porites lobata* (Cebu, Philippines). Coral Reefs 3:87–90
Pätzold J (1986) Temperature and CO_2 changes in tropical surface waters of the Philippines during the past 120 years: record in the stable isotopes of hermatypic corals. Berichte Geol-Paläont Inst Universität Kiel 12:1–92 (in German)
Quinn TM, Crowley TJ, Taylor FW (1996) New stable isotope results from a 173-year coral record from Espititu, Vanuatu. Geophys Res Lett 23:3413–3416
Reiss Z, Hottinger L (1984) The Gulf of Aqaba: ecological micropaleontology. Springer, Berlin Heidelberg New York
Ritchie JC, Eyles CH, Haynes CV (1985) Sediment and pollen evidence for an early to mid-Holocene humid period in the eastern Sahara. Nature 314:352–355
Rohling EJ, Bigg GR (1998) Paleosalinity and $\delta^{18}O$: a critical assessment. J Geophys Res 103:1307–1318
Shemesh A, Luz B, Erez J (1994) Carbon isotopes, dissolved oxygen, and the carbonate system in the northern Gulf of Aqaba (Elat). Isr J Earth Sci 43:145–155
Shen C-C, Lee T, Chen C-Y, Wang C-H, Dai C-F, Li L-A (1996) The calibration of D[Sr/Ca] versus sea surface temperature relationship for *Porites corals*. Geochim Cosmochim Acta 60:3849–3858
Swart PK (1983) Carbon and oxygen isotope fractionation in scleractinian corals: a review. Earth Sci Rev 19:51–80
Swart PK, Leder JJ, Szmant AM, Dodge RE (1996) The origin of variations in the isotopic record of scleractinian corals, II. Carbon Geochim Cosmochim Acta 60:2871–2885
Weber JN, Woodhead PMJ (1972) Temperature dependence of oxygen-18 concentration in reef coral carbonates. J Geophys Res 77:463–705
Wefer G, Berger WH (1991) Isotope paleontology: growth and composition of extant calcareous species. Mar Geol 100:207–248
Weiss H, Courty M-A, Wetterstrom W, Guichard F, Senior L, Meadow R, Currnow A (1993) The genesis and collapse of third millennium north Mesopotamian civilisation. Science 261:995–1004
Wellington GM, Dunbar RB, Merlen G (1996) Calibration of stable oxygen isotope signatures in Galápagos corals. Paleoceanography 11:467–480
Westendorf W, Henfling E (1989) Das Klima im Alten Ägypten nach Hieroglyphen-aufzeichungen. In: Klimaforschungprogramm des Bundesminsterium für Forschung und Technologie "Statusseminar", pp 493–494
Wolf-Vecht A, Paldor N, Brenner S (1992) Hydrographic indications of advection/convection effects in the Gulf of Elat. Deep-Sea Res 39:1393–1401